A summer phytoplankton bloom triggered by high wind events in the Labrador Sea, July 2006

Yongsheng Wu,[1] Trevor Platt,[1] Charles C.L. Tang,[1] Shubha Sathyendranath,[1,2] Emmanuel Devred,[1] and Shue Gu[1]

Received 6 February 2008; revised 10 April 2008; accepted 21 April 2008; published 28 May 2008.

[1] The mechanisms of nutrient resupply for an episodic phytoplankton bloom observed in the central Labrador Sea in July 2006 were investigated. Two physical processes, mixed-layer deepening and Ekman pumping, are proposed to account for the implied nutrient replenishment. The nutrient flux and chlorophyll concentration before and during the bloom were estimated from a simple coupled nitrate-phytoplankton model. The model results show that the enrichment of nutrients in the euphotic layer and the subsequent bloom were related to two wind events (storms) in the period July 7–10. As the mixed layer deepened, nutrient from below the nitricline were entrained into the euphotic zone. The Ekman pumping, which was most intense at the storm centre, enhanced the transport of the nutrients by raising the nitricline. However, Ekman pumping alone was not able to transport sufficient nitrate to the euphotic layer to support the observed phytoplankton bloom. **Citation:** Wu, Y., T. Platt, C. C. L. Tang, S. Sathyendranath, E. Devred, and S. Gu (2008), A summer phytoplankton bloom triggered by high wind events in the Labrador Sea, July 2006, *Geophys. Res. Lett.*, *35*, L10606, doi:10.1029/2008GL033561.

1. Introduction

[2] In temperate latitudes, the onset of stratification in the spring initiates the annual bloom of phytoplankton, which then usually continues until nutrients in the surface mixed layer become depleted. After the spring bloom, primary production is dependent on recycled nutrients, and further blooms of phytoplankton are not possible unless and until nutrients are re-supplied to the surface layer. The re-supplied nutrients are characterized as new nutrients [*Dugdale and Goering*, 1967] and the associated primary production as new production.

[3] Typically, there are two general mechanisms for nutrient resupply after the annual spring bloom. The first is turbulent vertical mixing. When the water column is stratified, the transport of the deep layer with rich nutrient water into the upper layer is blocked by the density gradient. Thus, the new nutrient re-supply becomes difficult unless some physical processes, such as vertical mixing induced by storms, are strong enough to penetrate the pycnocline and entrain the nutrients into the euphotic layer [*Iverson et al.*, 1974]. The other potential mechanism is wind-induced coastal upwelling and Ekman pumping [*McClain and Firestone*, 1993].

[4] Using satellite data, the response of chlorophyll fields to storms and the correlations between the wind fields and changes in surface chlorophyll concentration have been studied by many investigators [*Platt et al.*, 2005; *Son et al.*, 2006]. In this paper, we use a simple coupled nitrate-phytoplankton model to simulate the observed bloom, and from the model results, investigate the mechanisms of new nutrient supply.

2. Observations of A Phytoplankton Bloom in July 2006

[5] In the central Labrador Sea, the annual spring bloom starts around the middle of May when the thermal stratification is established, and ends around the middle of June when nutrients in the euphotic zone become depleted. After the end of the bloom, the chlorophyll concentration is a fraction of the value during the bloom. The summer is usually a period of relatively low phytoplankton growth. However, in mid-July 2006, when the annual spring bloom was already over, an intense bloom over a large part of the central Labrador Sea (hereafter referred to as the episodic bloom) was observed in satellite images. Figures 1a and 1b show the weekly composites of chlorophyll-a concentration in 8–23 July 2006, which are derived from the daily Moderate Resolution Imaging Spectroradiometer (MODIS) data with a spatial resolution of 1.5 × 1.5 km. The bloom started at 51.6°W, 58.2°N in the second week of July, and spread westward and southward over a period of 3 weeks. Our study focuses on the bloom area enclosed by the box in Figure 1. The algae species analysis (the diatom index) is shown in Figure 1c. This index, derived from the algorithm of *Sathyendranath et al.* [2004], indicates for each pixel in a composite image the probability that the phytoplankton community was dominated by diatoms during the bloom [*Stuart et al.*, 1998]. Although it is generally believed that the spring bloom in this area is dominated by diatoms, the observation of such an extensive diatom bloom in the summer is somewhat unexpected. Stimulation of diatom growth is the expected response to the supply of new nutrients. Figure 1d presents the time series of weekly chlorophyll concentration averaged over the box. The episodic bloom occurred after the annual spring bloom. It also shows that both the rate of increase and the magnitude of the bloom were higher than those of the spring bloom.

3. Wind Conditions and Ekman Pumping

[6] Using data from the Quick Scatterometer (QuikScat) satellite, we examined wind conditions in the Labrador Sea

[1]Coastal Ocean Science, Bedford Institute of Oceanography, Dartmouth, Nova Scotia, Canada.
[2]Plymouth Marine Laboratory, Plymouth, UK.

0094-8276/08/2008GL033561

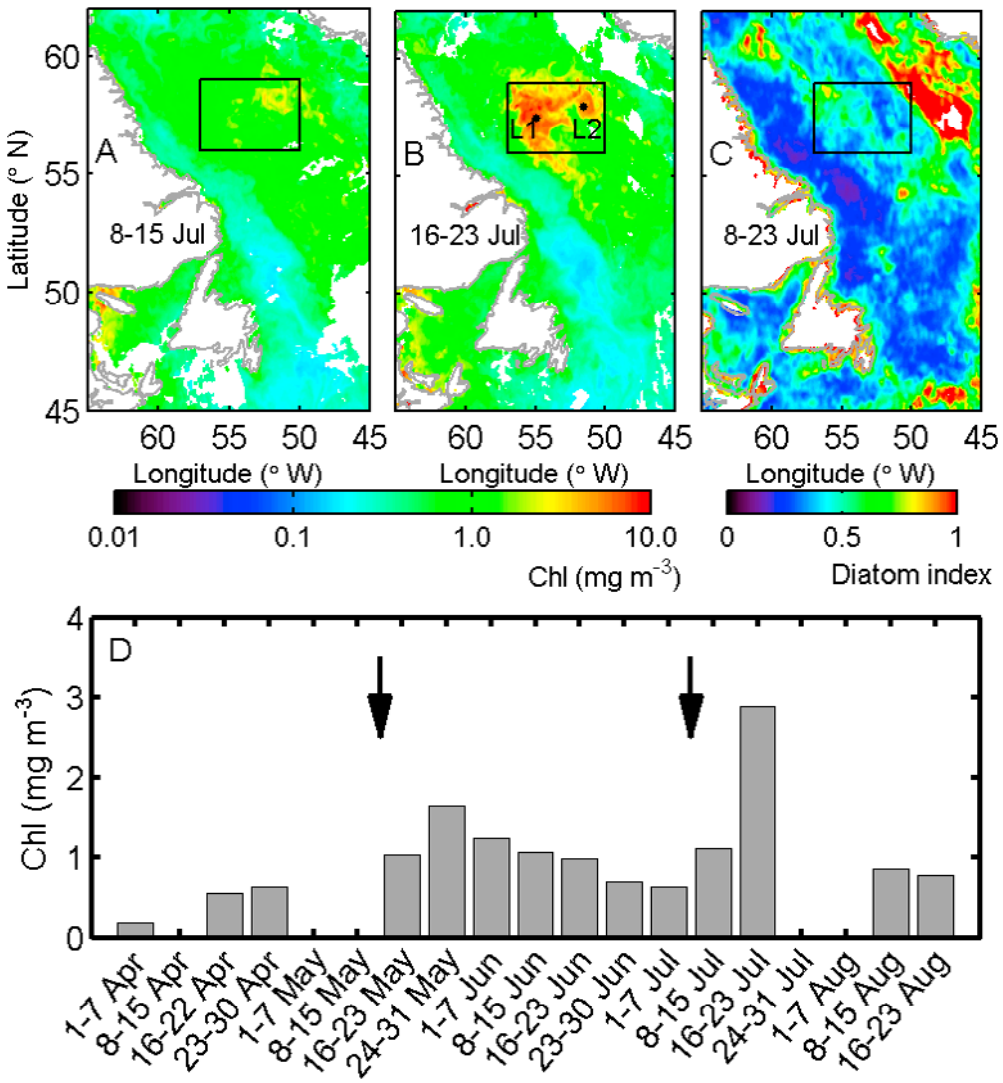

Figure 1. Composites of remotely-sensed data from (a) the second and (b) the third week of July, 2006. The box denotes the study area. The black dots in Figure 1b denote the locations of L1 and L2 used in Figure 3. (c) Diatom index (0 – 1) for 8–23 July, 2006. (d) Weekly mean chlorophyll concentration averaged over the box. The two arrows indicate the initiation of the spring bloom and the summer bloom. The blanks of the plotting present that there is no data due to the cloud coverage.

in July, and found two major wind events occurring in the two weeks prior to the bloom. Figure 2 shows the wind fields for July 7–10 and the derived Ekman pumping velocities (w_d) at the base of the Ekman layer calculated from the divergence of surface shear stresses [*McClain and Firestone*, 1993]. The spatial patterns show two strong upwelling areas on July 7 and 10 and both are in the bloom region.

[7] During the first wind event (July 7–8), strong winds blow over the western part of the bloom area (see Figure 1b). The area with high wind speeds (20 – 28 m s^{-1}) overlays the western part of the bloom area. Intense upwelling occurs in the area with high gradients of the wind speeds. The vertical velocity exceeds 150 $\times$ 10^{-6} m s^{-1} (13 m day^{-1}). The second wind starts in the morning of 10th. The horizontal pattern of the wind field is characteristic of a cyclonic storm. The wind speeds are low (<15 m s^{-1}) compared to those during the first wind event. The location, where the bloom started, matches well with the center of the cyclone (Figure 2). At the center, the vertical velocity reaches 180 $\times$ 10^{-6} m s^{-1} (16 m day^{-1}).

4. Model

[8] Based on the NPZD model of *Denman and Peña* [1999], we constructed a 1-D model in which only the N and P components were considered. The model is employed to simulate the observed bloom with the aim of understanding the mechanisms of nutrient resupply. In the model, the nutrient (e.g., nitrate, N) is controlled by mixing, vertical advection (Ekman pumping) and phytoplankton uptake. The change in phytoplankton concentration (P) is balanced by growth, vertical mixing, vertical advection and loss. The vertical mixing is parameterized by the vertical diffusion coefficient, which is obtained from the 2.5 level turbulence-closure model of *Mellor and Blumberg* [2004].

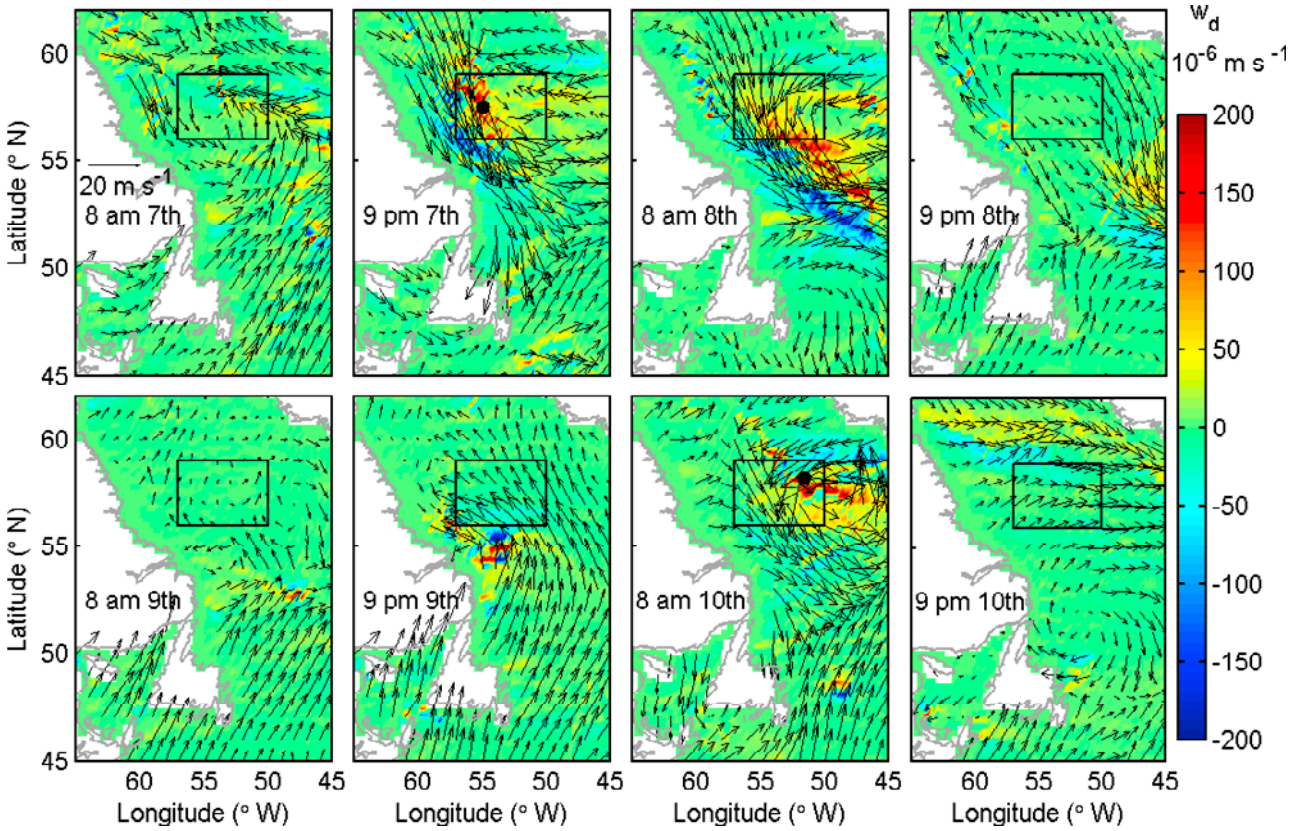

Figure 2. Wind fields and the Ekman velocity at the base of the Ekman layer for two storms in 7–12 July, 2006. Vectors are the wind velocities, and the color contour is the Ekman velocity (unit is 10^{-6} m s^{-1}). The black dots in the 9 pm 7th and 8 am 10th plots denote the locations of L1 and L2, respectively.

[9] The calculation of the growth rate is based on a spectrally-dependent algorithm by *Sathyendranath et al.* [1989]. The two parameters in the primary production and irradiance relationship (*P-I* curve) are the assimilation number (in mg C (mg Chl)$^{-1}$ h^{-1}) and the initial slope (in mg C (mg Chl)$^{-1}$h^{-1}(W m^{-2})$^{-1}$), which are set to 2.2 and 0.08, respectively. The penetrating component of the total irradiance at the sea surface is calculated with the model of *Bird* [1984]. The half-saturation constant for nitrate uptake is 0.5 mmol N m^{-3}. The carbon chlorophyll ratio is 50 mg C (mg Chl)$^{-1}$. The loss rate, which represents the removal of the phytoplankton due to grazing, respiration and mortality, is set to 0.1 day^{-1}. The vertical profile of the vertical velocity associated with Ekman pumping is expressed as a function of water depth according to *Signorini et al.* [2001].

[10] The initial conditions of temperature and salinity required for the turbulence closure model are the monthly temperature-salinity climatologies obtained from an objective analysis of historical data. The model was forced by wind stresses computed from the 2-D wind fields (QuikScat) described in Section 3, and by heat and moisture fluxes calculated from the meteorological parameters obtained from Canadian Meteorological Centre.

[11] The initial vertical chlorophyll profile is assumed a Gaussian distribution with the surface value determined by the satellite data. For nitrate, a simple two-layer structure is assumed with uniform distribution in each layer. We assume that the nitrate concentrations above and below the nutricline are 0.5 mmol m^{-3} and 10.0 mmol m^{-3}, respectively, according to the data of *Garcia et al.* [2006]. The Garcia et al. data are monthly and seasonal averages of historical data. The maximum and minimum nitrate concentrations occur in March and September, respectively. High vertical gradients are found between 20 m and 50 m. Because of the coarse resolution of the data set, the nitricline depth is not well defined. The nitricline depth in the model, 27 m, was obtained by tuning the value to give good agreement with the chlorophyll data. The sensitivity of the model results to the nitricline depth will be discussed in Section 5.2. The model was integrated for each 0.5° × 0.5° square in the area 65°W to 45°W, and 45°N to 62°N from 6 July to 25 July. There are 80 vertical levels. The resolution of the top 40 levels is 1 m. Below 40 m, the resolution increases exponentially to a maximum of 470 m at 3000 m depth. The time step is 1 minute.

5. Results

5.1. Vertical Structures

[12] The vertical distributions of density (relative to surface density), nitrate and chlorophyll as a function of time at locations L1 and L2 (Figure 1) from the model (Figure 3) show significant increases in the nitrate concentration immediately after the wind event in the period from July 7 to 9 in the upper layer at both locations, in particular at L1 because of the higher wind speeds there.

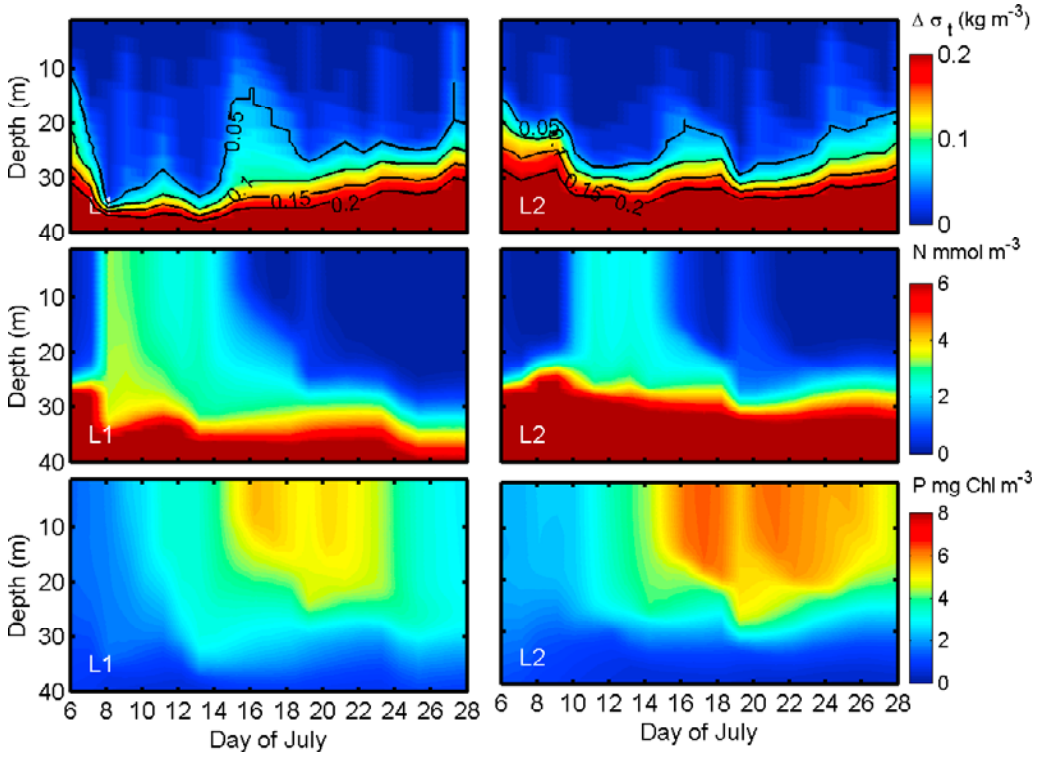

Figure 3. Vertical structures of density difference (from surface) $\Delta\sigma_t$, nitrate (N) and chlorophyll (P) at (left) L1 and (right) L2.

[13] Two processes are responsible for the increase of nitrate at L1 - turbulent mixing and Ekman pumping. The relative density (top plots) can be used to define the mixed-layer depth. If we use the value 0.1 kg m^{-3} as the criterion, the mixed-layer depth increased by about 10 m at L1 after the first wind event on July 8. The middle plots show that the nitricline is disturbed by the deep penetration of turbulent mixing. After the wind events, the mixed layer shallows. Around 16 July, the surface chlorophyll concentration reaches 5 mg m^{-3} at L1. At this concentration, the bloom can be clearly seen in the satellite images (Figure 1). Accompanying the rapid increase in chlorophyll is a sharp decrease in nitrate (middle plot).

[14] In contrast to the condition at L1, the nitricline at L2 does not deepen, but becomes shallower after the wind events of July 8–10. This indicates that the intensity of mixing is not strong enough to counter the effect of upwelling. It should be noted that the contribution of the horizontal advection is not considered in the 1–D model. In a 2–D ocean, the relaxation of the nutricline following the passage of a storm can cause the nutricline to oscillate at the inertial frequency [*Wu et al.*, 2007]. The effect of such oscillation to the net vertical transport of nutrient is expected to be small.

[15] On July 9, there is a rapid increase in the vertical velocity, which gives rise to a dome in the nitricline at L2 (Figure 3, middle plot). The upward movement of the nitrate by Ekman pumping in conjunction with vertical mixing causes the increase of the nitrate at L2 in July 15. The decrease in chlorophyll concentration in July 19, which is particularly pronounced at L2 (Figure 3), is related to a wind event on that date. The model results (Figure 3) indicate that both Ekman pumping and vertical mixing are responsible for the nitrate replenishment. A detailed analysis of the relative contribution of these two physical processes will be given in Section 5.3.

5.2. Horizontal Patterns

[16] The horizontal patterns of the mean surface chlorophyll in the second (8–15 July) and third (16–23 July) weeks of July from the model (Figure 4) show that the physical processes can account for the bloom observed in the satellite data (Figures 1a and 1b). At L1 and the surrounding area where the bloom is most intense, the chlorophyll concentration from the model is in the range 4 – 8 mg m^{-3} in general agreement with the observation. However, an obvious disagreement is in the south of the study area (54°N), where the model overestimates the chlorophyll concentration. Possible causes of the disagreement include over-simplification of the biological model, errors in the wind data and uncertainty in the horizontal distribution of nitrate in the Labrador Sea. Here we examine the sensitivity of the model to nitricline depth by increasing the initial nitricline depth from 27 m to 37 m for a location south of the study area, L3 (see Figure 4 for the location). Such an increase is consistent with the data of *Garcia et al.* [2006], which show that the nitricline depth in the Labrador Sea increases from northwest to southeast reaching a maximum of around 50 m south of Greenland. With a deeper nitricline, the mean surface chlorophyll concentration at L3 for July 16–23 is reduced from 8 mg m^{-3} to 3 mg m^{-3}. This suggests that the lack of horizontal variation in the nitrate profiles in the model may explain the discrepancy between the model and the data south of the study area.

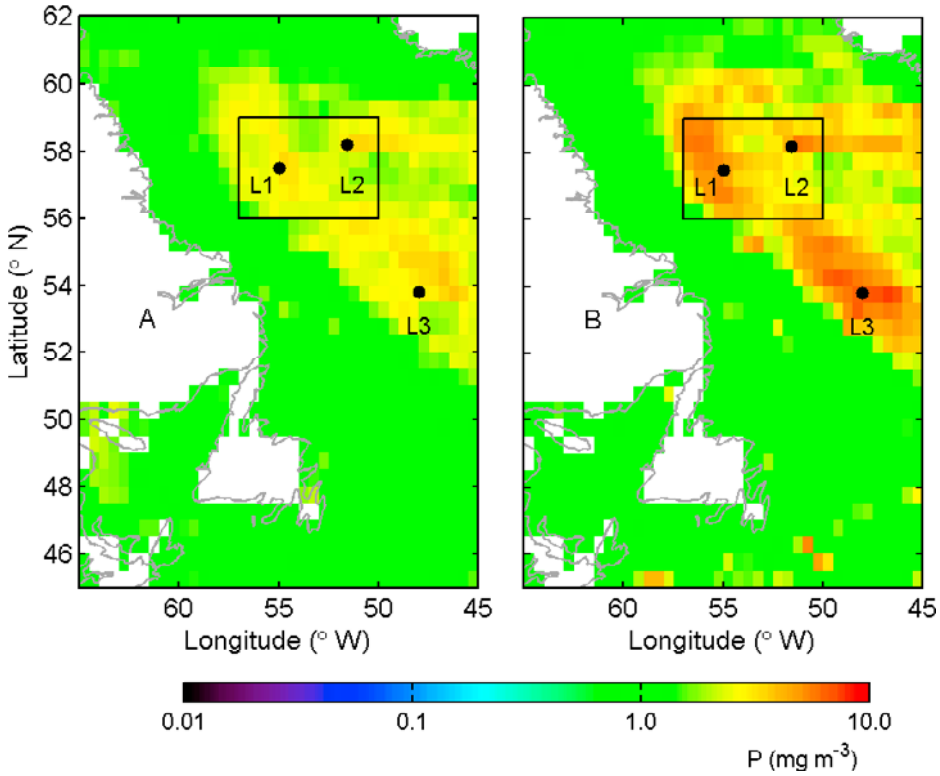

Figure 4. Horizontal distributions of the surface chlorophyll concentration from the model: (a) 8–15 July average and (b) 16–23 July average.

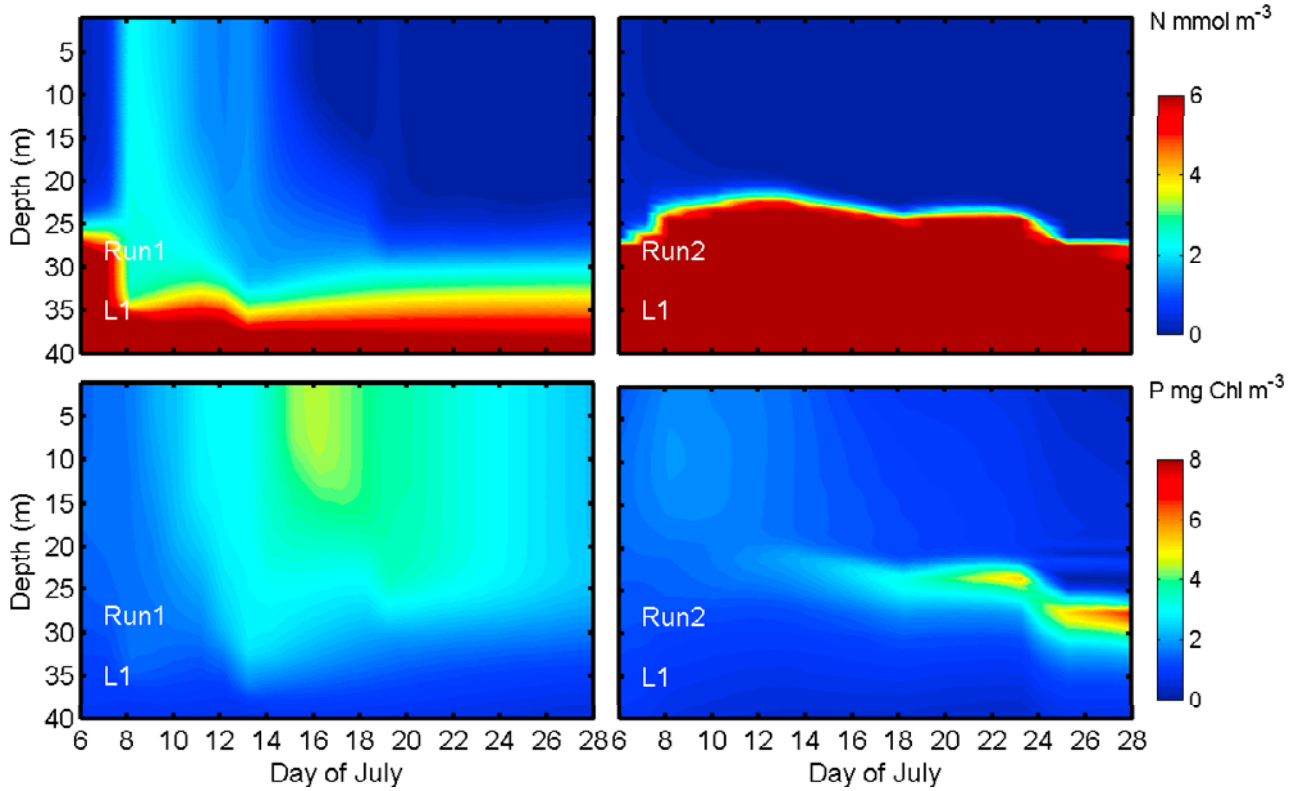

Figure 5. Model vertical structures of nitrate (N) and chlorophyll (P) at L1 from (left) Run 1 and (right) Run 2.

5.3. Contributions from Mixing and Upwelling

[17] The relative contributions of turbulent mixing and upwelling to nitrate replenishment were investigated from two sensitivity runs for L1 in which mixing and Ekman pumping were considered separately. In Run 1, the vertical velocity was set to zero (no Ekman pumping). In Run 2, the diffusion coefficient was set to zero (no vertical mixing).

[18] The left plots of Figure 5 (Run 1) show the nitricline is slightly deeper than that in the base run (Figure 3). Since the vertical velocity is zero, the upward transport of nutrients into the upper layer by mixing is not enhanced. The result is a slower phytoplankton growth in comparison to the base run. In Run 2, the nitricline is shallower than that in the base run as well. However, the nitrate concentrations in the surface layer are much lower than those in the base run because the principal mechanism to transport the nitrate to the surface is vertical mixing, which is absent in Run 2. The highest chlorophyll concentration occurs around the nitricline. This is the depth at which both nutrient and irradiance are available. From a comparison of Figures 3 and 5, we find that Ekman pumping alone is not able to transport sufficient nitrate to the euphotic layer to support the observed phytoplankton bloom. However, upwelling can reinforce the effect of mixing if the vertical velocity during the upwelling event is high. High vertical velocities are usually associated with intense cyclones or storms as shown in Figure 2.

6. Conclusions

[19] The enrichment of nutrients in the euphotic layer and the subsequent occurrence of the bloom observed in satellite data are related to two wind events (storms) in 7 – 10 July, during which the nutrients below the nitracline were entrained into the euphotic layer by vertical mixing and Ekman pumping. The Ekman pumping enhances the vertical transport of the nutrients by raising the nitricline and by advecting the nutrients upward. However, Ekman pumping alone could not account for the nutrient re-supplied to support the observed phytoplankton bloom. We conclude that, under the influence of strong winds, both entrainment by mixed-layer deepening and Ekman pumping were implicated as stimuli for the summer bloom, the relative importance of each mechanism varying with location across the study area.

[20] **Acknowledgments.** The research has been supported by Canadian Space Agency under the Ocean's Pulse (TOP) project. The authors thank C. Hannah and B. Greenan for reading an early version.

References

Bird, R. E. (1984), Simple, solar spectral model for direct-normal and diffuse horizontal irradiance, *Sol. Energy*, *32*(44), 461–471.

Denman, K. L., and M. A. Peña (1999), A coupled 1-D biological/physical model of the northeast subarctic Pacific Ocean with iron limitation, *Deep Sea Res., Part II*, *46*, 2877–2908.

Dugdale, R. C., and J. J. Goering (1967), Uptake of new and regenerated forms of nitrogen in primary productivity, *Limnol. Oceanogr.*, *12*, 196–206.

Garcia, H. E., et al. (2006), World Ocean Atlas 2005, *vol. 4, Nutrients, NOAA Atlas NESDIS 64*, 396 pp., NOAA, Silver Spring, Md.

Iverson, R. L., et al. (1974), Summer phytoplankton blooms in Auke Bay, Alaska, driven by wind mixing of the water column, *Limnol. Oceanogr.*, *19*, 271–278.

McClain, C., and J. Firestone (1993), An investigation of Ekman upwelling in the North Atlantic, *J. Geophys. Res.*, *98*, 12,327–12,340.

Mellor, G. L., and A. F. Blumberg (2004), Wave breaking and ocean surface layer thermal response, *J. Phys. Oceanogr.*, *34*, 693–698.

Platt, T., et al. (2005), Physical forcing and phytoplankton distributions, *Sci. Mar.*, *69*, 55–73.

Sathyendranath, S., et al. (1989), Remote sensing of oceanic primary production: Computations using spectral model, *Deep Sea Res.*, *36*, 431–453.

Sathyendranath, S., et al. (2004), Discrimination of diatoms from other phytoplankton using ocean-colour data, *Mar. Ecol. Prog. Ser.*, *272*, 59–68.

Signorini, S. R., et al. (2001), Seasonal and interannual variability of phytoplankton, nutrients, TCO_2, pCO_2 and O_2 in the eastern subarctic Pacific (ocean weather station Papa), *J. Geophys. Res.*, *106*, 31,197–31,215.

Son, S., et al. (2006), Satellite observation of chlorophyll and nutrients increase induced by Typhoon Megi in the Japan/East Sea, *Geophys. Res. Lett.*, *33*, L05607, doi:10.1029/2005GL025065.

Stuart, V., et al. (1998), Pigments and species composition of natural phytoplankton populations: Effect on the absorption spectra, *J. Plankton Res.*, *20*(2), 187–217.

Wu, Y., et al. (2007), Short-term changes in chlorophyll distribution in response to a moving storm: A modeling study, *Mar. Ecol. Prog. Ser.*, *335*, 57–68.

E. Devred, S. Gu, T. Platt, S. Sathyendranath, C. C. L. Tang, and Y. Wu, Coastal Ocean Science, Bedford Institute of Oceanography, Dartmouth, NS B2Y 4A2, Canada. (wuy@mar.dfo-mpo.gc.ca)